=== **MARINE PHYSICS** ===

Variability of Internal Tides in the Coastal Water Area of Oahu Island (Hawaii)

V. G. Bondur[a], Yu. V. Grebenjuk[a], and K. D. Sabinin[b]

[a]Aerokosmos Scientific Center for Aerospace Monitoring, Moscow, Russia
[b]Space Research Institute, Russian Academy of Sciences, Moscow, Russia
E-mail: vgbondur@online.ru
Received February 6, 2007; in final form, July 16, 2007

Abstract—The variability of the parameters of semidiurnal internal tides in Mamala Bay (Oahu Island, Hawaii) was investigated using the experimental data obtained with ADCP bottom current profilers and thermistor strings. It was stated that the size, shape, and orientation of the orbits, as well as the sign of the rotation of the orbital currents, are rarely similar to those characteristic of progressive internal waves on a rotating Earth. It is supposed that such unusual features of the orbital currents are related to the interference of the waves that arrive from the straits rimming Oahu Island and to the waves that, under favorable conditions, are episodically generated at the shelf edge of Mamala Bay. Due to the fact that the floor inclinations of the shelf in the bay are supercritical for semidiurnal internal tides, the local generation of internal tides is poorly efficient.

INTRODUCTION

Internal tides (IT) generated over irregularities of the bottom topography represent the principal source of energy for mixing the waters of a stratified ocean [17]. The area studied is located in the region of the Hawaiian Ridge, which features steep slopes and is the site of the most intensive generation of IT. Due to this reason, here, comprehensive IT measurements within the frameworks of the HOME program are performed [5, 12, 15, 16]. However, despite the intensive studies of IT according to this program and in earlier experiments [18], many issues are still unclear because of the extreme complexity of the IT field in the region of the Hawaiian Ridge and, especially, in Mamala Bay of Oahu Island (Fig. 1). The principal particular feature of this ridge is the overcritical (for the semidiurnal waves dominating here) steepness of its slopes: therefore, the IT are usually generated at significant depths.

Taking into account the fact that the bottom inclination at the shelf edge in the bay is overcritical for the mean density stratification, it is assumed that here IT are generated at depths of 500–1000 m rather than over the shelf edge; at those depths, the rays of the semidiurnal IT (below, referred to as BBM2 waves), owing to the decreasing stratification, become steeper and coincide with the bottom inclination. Precisely from these depths of the critical inclination occurs the emission of the BBM2 waves; however, only toward the open ocean does the baroclinic upslope and the bottom inclination become greater than that of the rays.

Nevertheless, at the shelf edge of Mamala Bay, one observes significant BBM2 waves; in the publications available [5, 12, 15, 16], they are related to remote sources over swells in the straits on either side of Oahu Island.

Arriving to the bay, these waves form a complicated interference field variable not only in space but also in time owing to the changing background conditions. In particular, as will be shown below, the cyclonic rotation of the IT currents observed in the bay (noted but not explained in [18]), as well as the strong variability in the orbits of the currents sometimes reminding one of the orbits of Sverdrup waves, may be caused by this kind of wave interference. Similar to the surface tides, we will use this name to refer to free internal waves in which water particles rotate over anticyclonic orbits of elliptic shape with ratios of axes equal to the ratios of local inertial frequencies to wave frequencies.

In addition to the semimensular IT variations (assessed in [12]) characteristic for the tides, one also observes variability on other temporal scales, which may be related to the changes in the buoyancy frequency and in the currents both at the sites of wave generation and over the routs of their propagation to the site of the measurements [15].

Despite the great number of thorough experiments performed in the areas off Oahu Island and the comprehensive analysis of the field data obtained and the results of numerical modeling, the possibility of local generation of the BBM2 waves over the shelf edge in Mamala Bay proper owing to the strong variability of
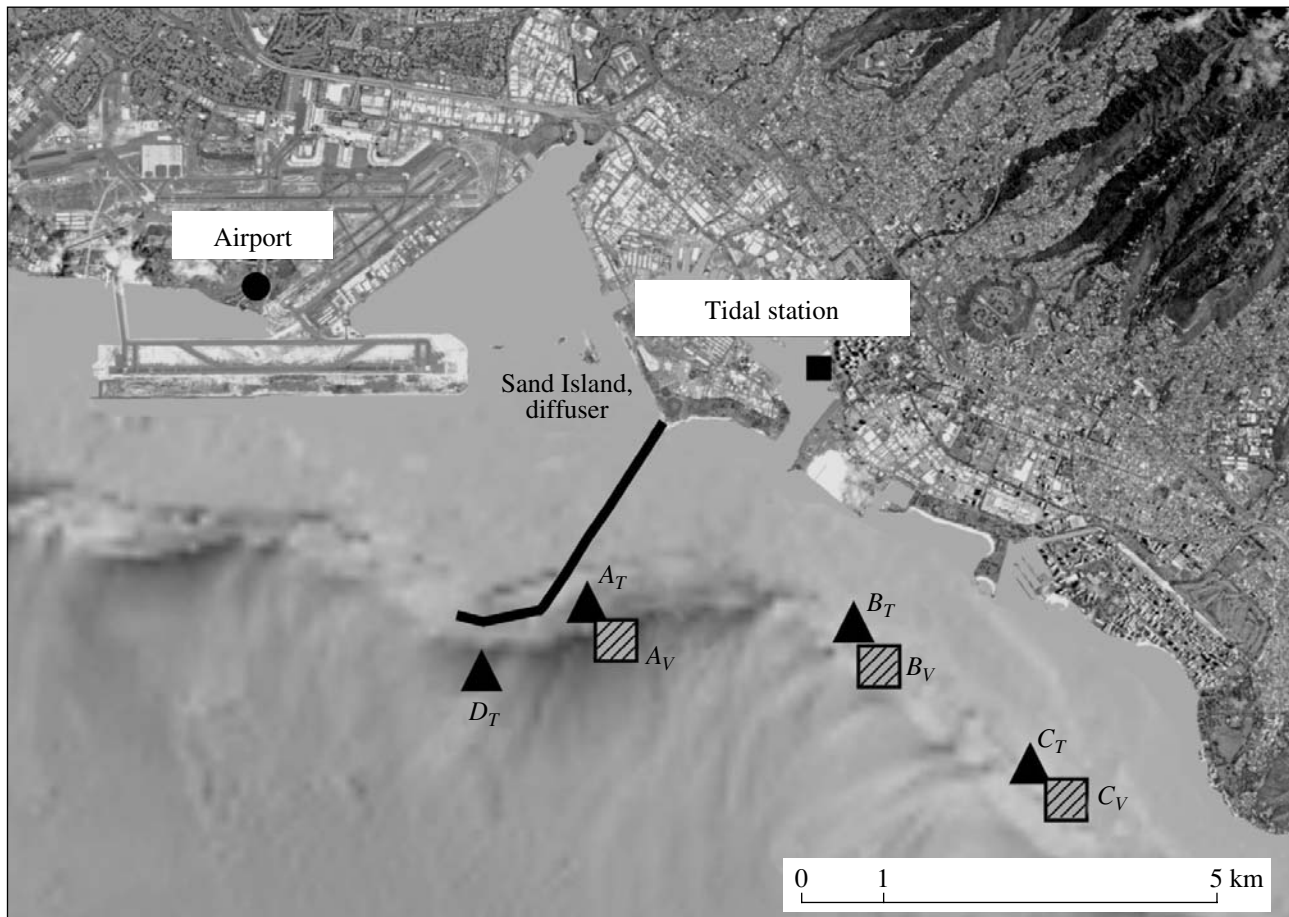
Fig. 1. Map of Oahu Island and the location of the stations of the measurements in Mamala Bay.

local stratification and currents in this region has remained beyond the scope of scientists' consideration.

Based on the data of the measurements of current and temperature variations on the shelf of Mamala Bay performed in August–September of 2002–2004 [1, 2, 7, 8, 10, 11, 14], we studied the particular features of the relatively small-scale IT variability that still remain beyond the scope of the research.

PARTICULAR FEATURES OF THE MEASUREMENTS AND EXPERIMENTAL DATA

In order to study the characteristics of the tidal internal waves on the shelf off Oahu Island, we used the results of the hydrophysical measurements performed in the area of Mamala Bay in 2002–2004 during the survey of anthropogenic impacts on the ecosystems of near-shore areas [1, 2, 3, 7–10, 11, 13, 14]. These studies included a survey of the area from spacecrafts and sea-truth measurements of the hydrophysical, biological, and chemical characteristics of the environment [1, 7].

The measurements of the hydrophysical characteristics of the environment were performed using a series of stationary stations supplied with thermistor strings and acoustic Doppler current profilers (ADCP), onboard measurements from ships with CTD and XBT sensors, and lowered and towed microstructure profilers (MSS) [7, 8, 10, 13]. In Fig. 1, one can see the location of the stationary stations in the bay at which measurements of the vertical temperature profiles (stations At, Bt, Ct, and Dt) and of the three components of the current vector (stations Av, Bv, and Cv) were carried out during 2–3 weeks. Below, in the description of the experiment, we will use numerals 3 and 4 after the literal names of the stations to denote the year of the measurements (2003 and 2004, respectively). When performing the measurements, the thermistor strings and ADCP profilers were located close to each other.

Figure 1 shows that the temperature and current measurements were made in three areas of Mamala Bay: immediately near the diffuser of the damping facility (stations A and D), at a distance of ~3.5 km east of it (stations Bt and Bv), and 7 km southeast of the diffuser (stations Ct and Cv). At the stationary stations, current measurements were performed within the depth range from 3.5 to 75.5 m with a depth step of 2 m and a time step of 1 min. The mea-

Measurements of hydrophysical parameters in Mamala Bay in 2003–2004

Year	2003	2004	2003	2004	2003	2004	
Acoustic Doppler profilers	Av		Bv		Cv		
Time of the measurements	31 Aug–22 Sep	–	31 Aug–22 Sep	20 Aug–8 Sep	31 Aug–22 Sep	23 Aug–8 Sep	–
Interval between the measurements, min	1	–	1	1	1	1	–
Depths, m	4.5–71.5	–	4.5–76.5	4.5–76.5	4.5–76.5	4.5–76.5	–
Thermistor strings	At		Bt		Ct		Dt
Time of the measurements	27 Aug–22 Sep	14 Aug–7 Sep	31 Aug–22 Sep	18 Aug–7 Sep	31 Aug–22 Sep	20 Aug–8 Sep	23 Aug–7 Sep
Interval between the measurements, min	5	0.5	2	0.5	2	0.5	0.5
Number of levels	15	8	7	8	6	8	18
Depths, m	3.5–45.5	17–80	22–66	19–76	20–62	21–70	23–172

surements of the water temperature were performed at different depths from 3–18 m to 45– 76 m with an interval of 2–5 min in 2003 and 30 s in 2004 [7, 10].

Information about these measurements is listed in the table. Owing to the step and duration of the measurements, the data obtained allow one to study the variability of the hydrophysical characteristics in Mamala Bay on scales from a few minutes to 20 days.

METHODS FOR EXPERIMENTAL DATA PROCESSING

The processing of the experimental data obtained included preliminary and special stages. The preliminary processing implied the following operations:

—formation of data massifs by the results of the measurements of the temperature (T) and current velocities (U, V) at stations A, B, and C;

—removal of "faulty" values;

—smoothing (low-frequency filtration) of the massifs in order to reduce the measurement errors with a subsequent increase in the temporal interval up to 1 h; and

—formation of data massifs according to the depths of the isotherm location from the results of the water temperature measurements at several levels (from 6 to 18).

For smoothing time series, a Butterworth filter of the 6th order with a cutting frequency of 2 cycle/h was applied. For smoothing over the vertical, a Butterworth filter of the 4th order with a cutting frequency of 0.5 cycle/m was used.

The special processing for the IT analysis from the temperature and current velocity profiles implied the calculation of the following characteristics:

—the barotropic (averaged over the vertical) and baroclinic (after removal of the barotropic ones) components of the current velocity U and V,

—the components of the baroclinic and barotropic currents in the frequency range of the semidiurnal tide M2 (band-pass Butterworth filter of the 6th order in the band from 0.07 to 0.09 cycle/h),
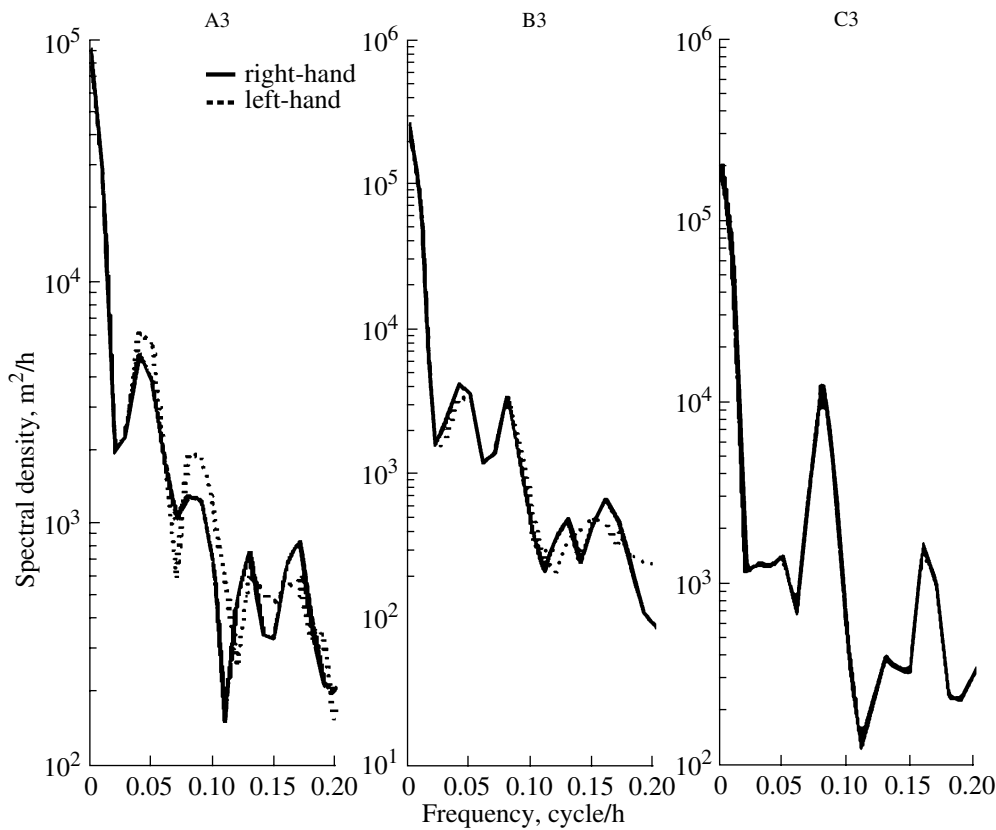
Fig. 2. Spectra of the rotation components at stations Av, Bv, and Cv in 2003 at a depth of 10 m.

—the components of the isotherm displacements in the frequency range of the semidiurnal tide,

—hodographs of the baroclinic and barotropic currents, and

—the mean spectra of variations of the currents and the vertical displacements of the isotherms.

The results of the processing are presented below.

MEAN CHARACTERISTICS OF THE CURRENTS, TEMPERATURE, AND STRATIFICATION IN MAMALA BAY

In Mamala Bay, the currents are mainly directed westward parallel to the coast [6, 16]. According to the data of our measurements in 2003–2004, the mean value of the velocity modulus in the layer deeper than 16 m was 11–18 cm/s [2, 8]. In the upper layer, owing to the wind action, the current velocities increased and, at a depth of 10 m, reached 45–65 cm/s in 2003 and 20 cm/s in 2004. Near the diffuser, the dominating directions of the currents in 2003 were 230°–280°, while, in 2004, they were 100°–150° and 240°–270° [2, 10].

In September 2003, the temperature stratification significantly differed from the conditions characteristic for 2002 and 2004 by the very deep position of the thermocline, whose axis was located at depths of 80–100 m, while, in the layer from the surface to a depth of 70 m, during most of the period of the observations, the water temperatures varied within a narrow range of 26 ± 0.5°C [8, 10]. During the experiments of 2002 and 2004, the thermocline was located at depths of 30–50 m and the water temperature near the diffuser at depths of 28–70 m changed from 22 to 28°C [8, 10].

In 2003, the mean values of the buoyancy frequency estimated using the data of microstructural profiling ranged within 5–9 cycle/h in the layer of 40–45 m, while, in 2004, this range was 5–15 cycle/h at depths of 30–75 m [10, 11, 14].

Let us consider the mean spectra of the current and temperature variations obtained by us as a result of the data processing; relevant examples are presented in Figs. 2 and 3. In Fig. 2, one can see the spectra of rotation components of the currents calculated from the results of the current measurements in 2003 at stations Av–Cv at a depth of 10 m. The spectra were calculated for the current components that had right-hand (clockwise) and left-hand (anticlockwise) rotations.

An analysis of the graphs presented in Fig. 2 shows that, in the mean spectra of the rotation components of the currents in the upper layer, the left-hand rotation at the M2 frequency either dominates or equals the right-hand rotation, which is contrary to the pattern that should be observed for Sverdrup waves. This indicates either a left-hand rotation or reciprocal currents.

An analysis of the spectra of the rotation components of the currents calculated by the results of 2003 showed that, at all the frequencies, the oscillations during this year were weaker than those during 2004, though they featured the same character. The currents at site C3 were almost fully reciprocal as proved by the equality between the spectra of the right-hand and left-hand rotations (see Fig. 2).

Since the measurements of the vertical velocity component with the use of ADCP are imperfect, especially at low frequencies, we calculated the velocity spectra of the vertical displacements of the isotherms. The data were preliminarily smoothed with a filter of the 4th order with a cutting frequency of 20 cycle/h.

Figure 3 shows the spectrum of the vertical displacements of isotherms at site B4 obtained using the measurements performed in 2004. As one can see from the figure, the peaks of the spectral energy are observed at the frequencies that correspond to the semidiurnal and quarterdiurnal oscillations. Smaller peaks were
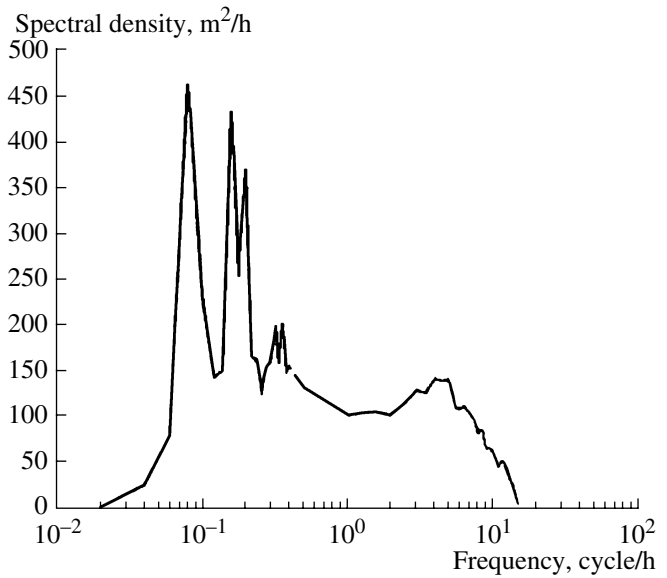

Fig. 3. Spectrum of the vertical velocity of the isotherm displacement at site Bt in 2004.

also distinguished for the oscillations with periods of 3–5 h. In the high-frequency region of the spectrum, one observes a broad peak at a frequency of 4–5 cycle/h (see Fig. 3).
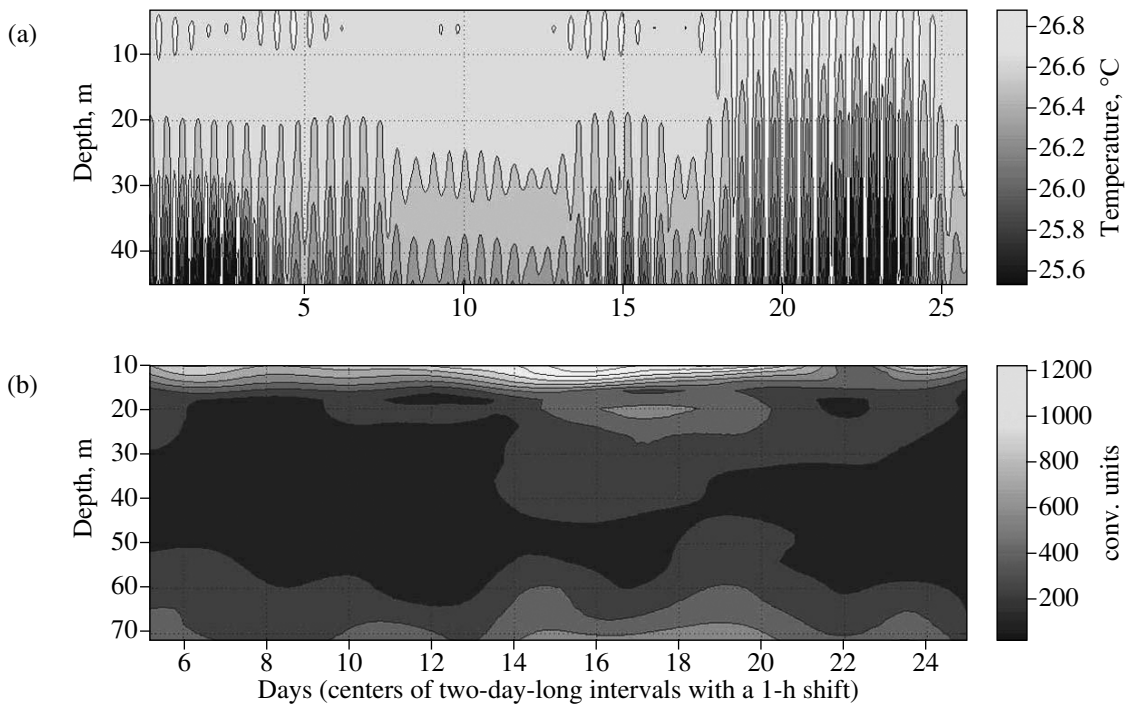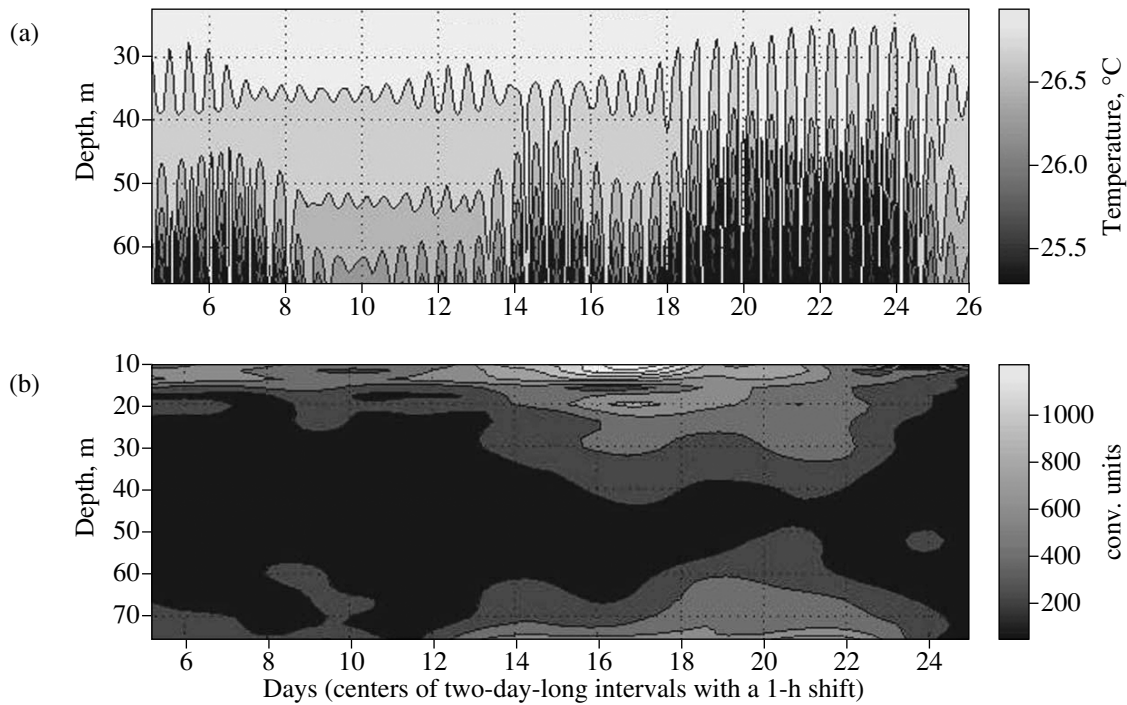

Fig. 4. Graphs of the variations of the (a) isotherms and (b) current intensity in the frequency range of the semidiurnal internal tide at station A in 2003.

Fig. 5. Graphs of the variations of the (a) isotherms and (b) current intensity in the frequency range of the semidiurnal internal tide at station B in 2003.

Let us now analyze the semidiurnal IT and their variability.

VARIABILITY OF THE INTENSITY OF SEMIDIURNAL INTERNAL TIDES

In order to study the characteristics of semidiurnal tides, in Mamala Bay, studies of the temporal variations of the isotherm depths and the amplitudes of the IT currents at different depths were performed.

Let us compare the variability of the intensity of the isotherm oscillations with that of the orbital currents in the IT by comparing the oscillations of isotherms and current amplitudes at the frequency of M2. The current amplitudes were estimated as the square root from the sum of the spectral amplitudes of the horizontal spectral components at the M2 frequency. Then, the amplitudes of the sliding spectra were calculated for overlapping 48-h intervals with a 1-h shift. As an example, Figs. 4a and 4b present the results of the calculations of the intensities of (a) the iosotherm oscillations and (b) current amplitudes at site A3 in 2003. The current amplitudes are represented by the values $(Su + Sv)1/2$ in conventional units, where Su and Sv are the spectra of the horizontal current components. An analysis of the graphs presented in Fig. 4 allows one to reach the following conclusions:

—The intensity of the IT strongly changes in time; the wave height may reach 40 m and higher (17th–19th days), while the currents are weak; the maximal currents (10th–15 days) are accompanied by lower waves (25 m).

—The outbursts in the oscillations of the current velocities and isotherms feature no semimensular inequality (one can rather recognize an 8-day periodicity) and do not coincide with each other in time.

—The strongest currents are confined to the upper layer; in the water column, they weaken and then slightly grow again near the bottom, which is natural when the lower mode dominates.

In 2003, a similar pattern was observed at site B3 (Fig. 5), though the disagreement between the intensity changes of the currents and the internal wave amplitudes, as well as the oscillations in the upper and lower layers, was manifested more clearly than at site A3. On days 18–20, the amplitude of the internal waves also reached 40 m. In the upper layer, in 2003, the ocean currents were the strongest on days 12–13, when the wave heights sharply decreased down to a few meters. Meanwhile, in the lower layer, the currents were generally weaker and reached their maximum only on days 16–17. On the whole, the domination of the lower mode here is less evident; on the other hand, one can recognize features of a ray mode of wave propagation.

Depth, m
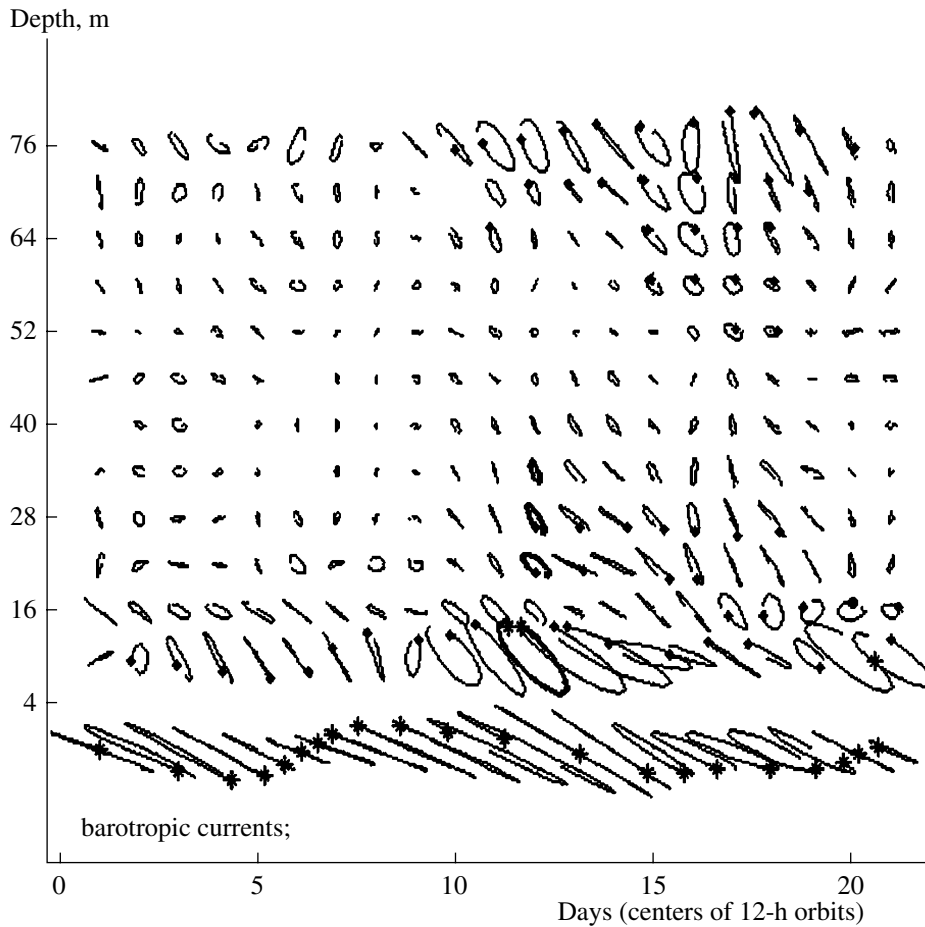
Fig. 6. Hodographs of the internal and barotropic (below) tides in the frequency domain of I2 at site Bv in 2003. The asterisks indicate the origins of the orbits.

A similar pattern of complicated and poorly compatible with each other changes in the oscillation intensity of isotherms and currents was also observed in 2004.

VARIABILITY IN THE HODOGRAPHS OF THE CURRENTS OF SEMIDIURNAL INTERNAL TIDES

The variations in the important parameters such as wave orbits virtually remained beyond the assessment in the publications available, though their unusual character (left-hand rotation [18]) was noted. In order to fill this gap, we will analyze the spatiotemporal variability in the hodographs of the internal tidal currents. Since the form of the hodograph (that is, the line circumscribed by the terminus of the current vector) coincides with the form of the trajectory over which water particles are transferred, hodographs well characterize the orbital motion of the water.

In the course of the experimental data processing, we plotted the hodographs of the currents of the IT

based on the results of the measurements at all the stations in 2003–2004. In Figs. 6 and 7, one finds examples of the hodographs of internal and barotropic M2 tides at stations B3 and C4. The daily-averaged wave orbits are plotted for depths of 10–76 m.

An analysis of the wave orbits showed that, in all the cases except site C3, the orbits of the M2 internal tide changed in time and space; only occasionally did they acquire the "correct" form typical of Sverdrup waves (Figs. 6, 7). The experimental data about the currents at site C3, where, at all the levels, almost exclusively reciprocal water motions were observed, seem to be questionable.

At station A3 (Fig. 6), the orbits that featured a right-hand rotation (days 12–13; the initial points of the orbits are indicated by asterisks) were observed only in a narrow region of the upper layer. A somewhat larger area with correct orbits was encountered at site C4 on the 7th–10th days of the observations, when the intensity of the baroclinic tidal currents reached its maximum. The correct and uniformly directed (along the
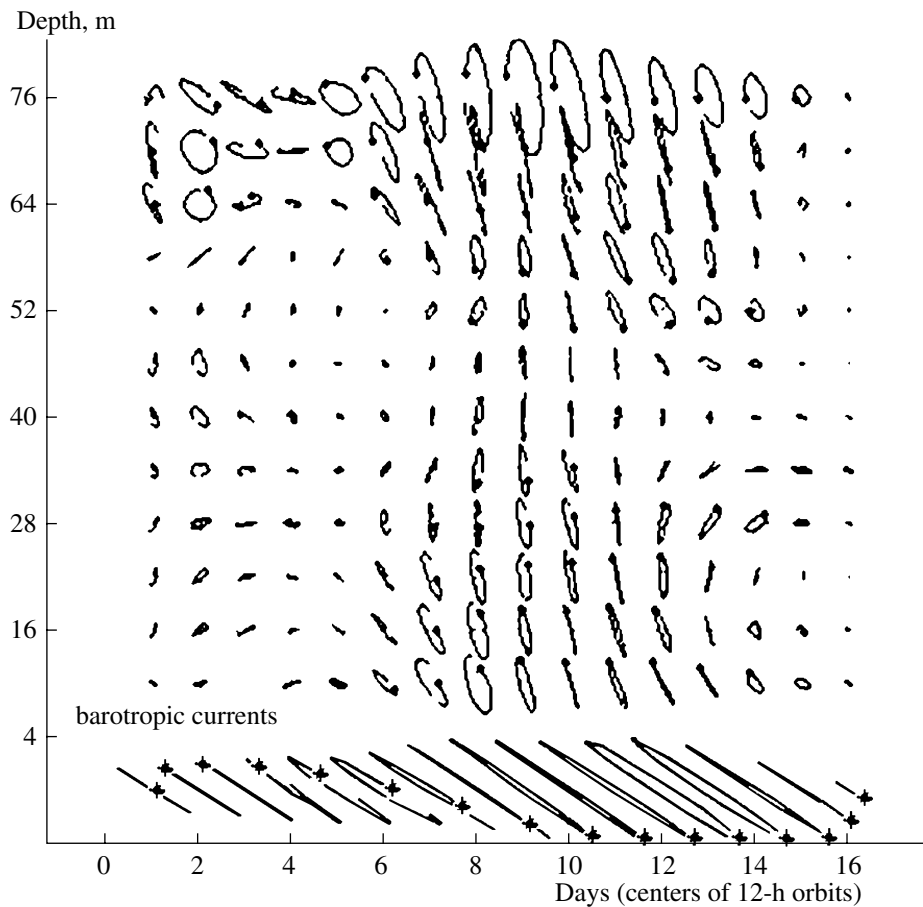
Fig. 7. Hodographs of the internal and barotropic (below) I2 tides at site Cv in 2004. The asterisks indicate the origins of the orbits.

meridian) orbits were observed almost throughout the entire water column and were enhanced near the surface and the bottom (Fig. 7). Meanwhile, the episodes with correct orbits were short-term and asynchronous; their directions in the upper and lower layers were different. In the middle of the water column, the orbits were smaller.

DISCUSSION OF THE RESULTS OF THE STUDIES OF INTERNAL TIDES

An analysis of the results of the processing performed allowed us to reveal the complicated spatiotemporal variability of the internal tide in Mamala Bay; it was characterized not only by the asynchronous character of the changes in the IT intensity at different depths and by the characteristic temporal scales of the variability (somewhat smaller than those of the regularity semimensular inequality) but also by break up of unusual character and sharp variability of the wave orbits.

The nonsimultaneous character of the changes in the intensity of the IT at different depths, in our opinion, may be regarded as a manifestation of the ray prop-

erties of the wave propagation in the variable medium. Indeed, despite the changes in the current amplitudes with depth characteristic for the lower mode, in this case, we may consider the domination of the ray type of wave propagation, in which the currents are also enhanced near the surface and the bottom but not simultaneously as should be for a mode standing with respect to the vertical. Moreover, the changes in the orientation and rotation of the current orbits with depth generally contradict the concept of a more or less correct lower mode.

It seems natural to relate the "dance" of the wave orbits observed to the interference of waves of different directions with variable parameters. Indeed, as a result of waves arriving from different directions, the orbits of the IT currents may strongly differ from the "correct" forms. As is known, correct orbits are extended in the direction of the wave propagation with a ratio between the minor and major axes of the orbit equal to $e = f/M2$ [4], where f is the Coriolis parameter. For the region considered, $e = 0.38$.

The orbit variability at the wave interference may be demonstrated by the example of coupling Sverdrup waves arriving from the east (wave 1) and from the northwest (wave 2), which is close to the situation observed in Mamala Bay. Let us define the current components of an elementary wave in the direction of its propagation and in the transverse direction as

$$U = a*\sin(M2*t + P), \quad V = a*e*\cos(M2*t + P),$$

where a is the amplitude, M2 is the frequency, and P is the phase.

The results of the calculations of the current orbits formed under the interaction of two regular waves with different amplitudes and phases are presented in Fig. 8, where the initial "correct" and coupled hodographs of the currents are shown for selected values of the amplitudes and phase differences between waves 1 and 2.

When waves with equal amplitudes and a phase difference of $P = 180°$ are coupled (Fig. 8a), the resulting orbit reminds one of the "correct" one, while, with the increase in the phase difference by $30°$ more ($P = 210°$), the orbit acquires a circular form retaining the "incorrect" rotation (Fig. 8b). At $a1/a2 = 1/2$ and a phase of $P = 240°$, the orbit elongates again but in the direction perpendicular to the case of $P = 210°$ and the current becomes virtually reciprocal (Fig. 8c).

Thus, the interference of waves of different directions not only allows one to judge about the wave direction from the orientation of the resulting orbits but also may change the direction of the current rotation and significantly distort the orbit form up to circular or reciprocal trajectories depending on the wave directions, amplitudes, and phases.

The domination of the left-hand current rotation of the internal as well as barotropic tides recognized by us was first mentioned in [12] and remained unexplained; most probably, it is related precisely to the superposition of waves from different directions. In so doing, if the density stratification and background currents change, the changes in the orbits are inevitable, which is well manifested in Figs. 4–8. One can readily see that, if the velocity of a wave 20 km long changes by only 20%, its phase changes by $30°$. The actual pattern is even more complicated because of the possible effect of boundary waves (such as, for example, Kelvin waves) and locally generated internal currents.

It is indicative that, in 2004, in the semidiurnal oscillations of the isotherms plotted according to the data of the thermistor strings installed at site D4 (Fig. 9) located somewhat below the shelf edge, one can readily notice an upward motion of the IT wave. This corresponds to the downward propagation of the energy of the inclined wave that was probably generated somewhat upslope on the shelf edge, which agrees with the
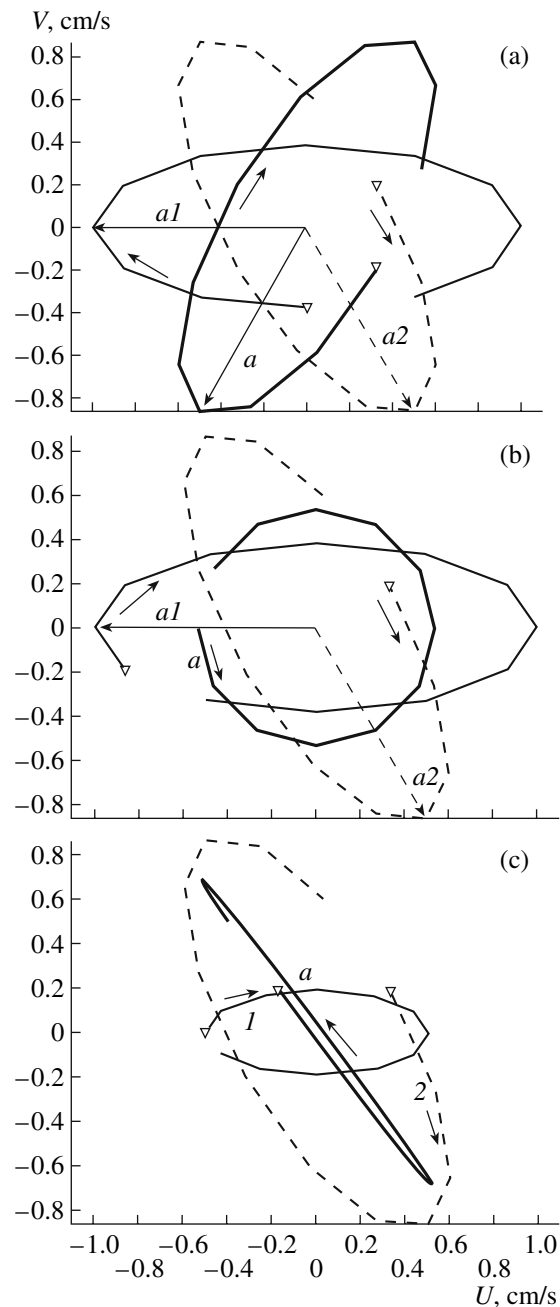
Fig. 8. Hodographs of the currents induced from coupling wave 1 (directed to the west, 270°) and wave 2 (directed at 150°) for different values of the amplitude ratios and phase differences: (a) $a1 = a2$, $P = 180°$; (b) $a1 = a2$, $P = 240°$; (c) $a1/a2$, $P = 240°$.

hypothesis about the significant role of the local wave generation.

CONCLUSIONS

Based on the analysis of the data of the temperature and current velocity measurements in Mamala Bay, we studied the variability of the characteristics of the semidiurnal internal tide. They helped to establish that
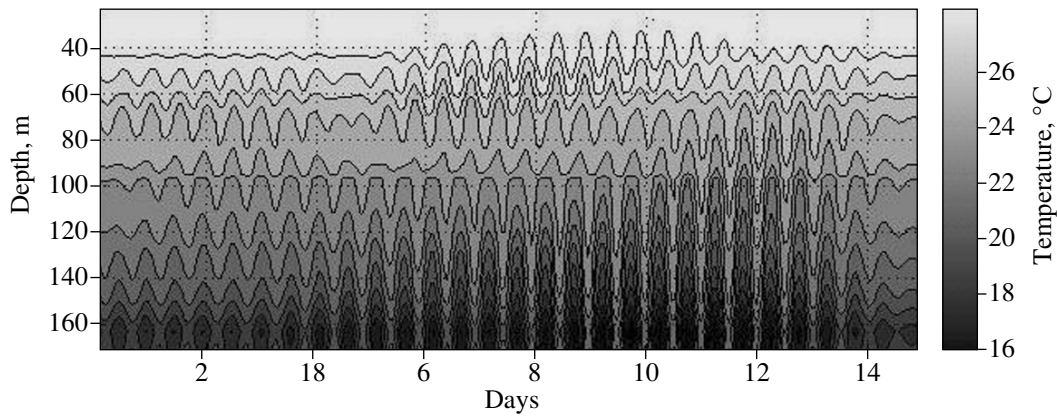
Fig. 9. Graph of semidiurnal isotherm oscillations at site Dt in 2004.

the amplitudes, forms, and orientations of the orbits, as well as the directions of the rotation of orbital currents of the IT, strongly vary in space and time. In so doing, the forms of the orbits and the directions of the rotation of the orbital currents only occasionally acquire features characteristic for progressive internal waves on a rotating Earth.

The facts established best fit the following pattern of the formation of the IT field on the shelf of the bay:

—The waves of the lower mode, which arrive from the straits and experience refraction on the sloping bottom, are coupled with the waves that are episodically generated on the shelf edge when the background conditions favorable for local generation are formed.

—The area considered is characterized by a moderate density stratification and overcritical bottom inclinations, which prevents wave emission from the shelf edge.

—Actually, the field of the internal tide here is probably formed not only by the waves arriving from afar as was believed earlier [5, 12, 15, 16, 18] but also by the waves of a local origin generated under the conditions favorable for this process.

—The background conditions also change along the paths of the propagation of IT coming from the straits, which results in the changes in the IT parameters and makes the spatiotemporal variability of the field even more complicated.

—The strong temporal variability in the hydrological conditions in the upper layer may cause a situation when, at selected moments, the bottom inclinations may be lower than the critical values and thus local IT generation on the shelf edge becomes possible.

—Despite the current amplitude changes with depth characteristic for the lower mode, which was observed in all the cases, one cannot infer about the absolute domination of the lower mode in the bay, since the cur-

rents enhance near the surface and the bottom under the ray type of wave propagation as well.

The nonsimultaneous character of the wave enhancement in the top and lower parts of the column and the changes in the orientation and rotation of the currents with depth are generally incompatible with the concept about the more or less correct lower mode. In this kind of wave field pattern, one can rather find manifestation of the ray type of propagation characteristic for the near-zone field of the internal tide.

In order to validate the hypothesis posed about the local generation of internal tides on the shelf edge of Mamala Bay, a thorough analysis of the current orbits and the vertical isotherm oscillations is required together with the characteristics of the changing background conditions. It is also important to make clear whether the Sverdrup waves that arrive from the strait are transformed into Kelvin waves over the steep continental slope of Oahu Island.

REFERENCES

1. V. G. Bondur, "Aerospace Techniques in Modern Oceanology," in *New Ideas in Oceanology. Vol. 1* (Nauka, Moscow, 2004) [in Russian].

2. V. G. Bondur, N. N. Filatov, Yu. V. Grebenyuk, *et al.*, "Studies of Hydrophysical Processes during Monitoringot Anthropogenic Impact on Coastal Basins Using the Example of Mamala Bay of Oahu Island in Hawaii," Okeanologiya **47** (6), 827–846 (2007) [Oceanology **47** (6), 769–787 (2007)].

3. V. I. Vedernikov, V. G. Bondur, M. E. Vinogradov, *et al.*, "Anthropogenic Influence on the Planktonic Community in the Basin of Mamala Bay (Oahu Island, Hawaii) Based on Field and Satellite Data," Okeanologiya **47** (2), 241–258 (2007) [Oceanology **47** (2), 221–237 (2007)].

4. K. V. Konyaev and K. D. Sabinin, *Waves Inside the Ocean* (Gidrometeoizdat, St. Petersburg, 1992) [in Russian].

5. M. H. Alford, M. C. Gregg, and M. A. Merrifield, "Structure, Propagation and Mixing of Energetic Baroclinic Tides in Mamala Bay," J. Phys. Oceanogr. **36**, 997–1118 (2006).

6. *Atlas of Hawaii, 3rd Edition* (University of Hawaii, Honolulu, 1998).

7. V. G. Bondur, "Complex Satellite Monitoring of Coastal Water Areas (Plenary Presentation)," in *Proc. 31st Int. Symp. on Remote Sensing of Environment* (St. Petersburg, 2006), pp. 1–6.

8. V. G. Bondur and N. N. Filatov, "Study of Physical Processes in Coastal Zone for Detecting Anthropogenic Impact by Means of Remote Sensing," in *Proceeding of the 7 Workshop on Physical Processes in Natural Waters* (Petrozavodsk, 2003), pp. 98–103 [in Russian].

9. V. Bondur and S. Starchenkov, Monitoring of Anthropogenic Influence on Water Areas of Hawaiian Islands Using RADARSAT and ENVISAT Radar Imagery in *Proc. 31st Int. Symp. on Remote Sensing of Environment* (St. Petersburg, 2006), pp. 184–187.

10. V. Bondur and M. Tsidilina, "Features of Formation of Remote Sensing and Sea truth Databases for The Monitoring of Anthropogenic Impact on Ecosystems of Coastal Water Areas," in *Proc. 31st Int. Symp. on Remote Sensing of Environment* (St. Petersburg, 2006), pp. 192–195.

11. C. Gibson, V. Bondur, R. Keeler, and Pak Tao Leung, "Remote Sensing of Submerged Oceanic Turbulence and Fossil Turbulence," Int. J. Dynamics of Fluids (IJDF) **2** (2), 111–135.

12. P. E. Holloway and M. A. Merrifield, "On the Spring-Neap Variability and Age of the Internal Tide at the Hawaiian Ridge," J. Geophys. Res. **108** (C4), 3126 (2003).

13. R. Keeler, V. Bondur, and D. Vithanage, "Sea Truth Measurements for Remote Sensing of Littoral Water," Sea Technology, No. 4, 53–58 (2004).

14. R. Keeler, V. Bondur, and C. Gibson, "Optical Satellite Imagery Detection of Internal Wave Effects from a Submerged Turbulent Outfall in the Stratified Ocean," Geophys. Res. Lett. **32**, L12610 (2005).

15. M. A. Merrifield and M. H. Alford, "Structure and Variability of Semidiurnal Internal Tides in Mamala Bay, Hawaii," J. Geophys. Res. **109** (C8), C05010 (2004).

16. M. A. Merrifield and P. E. Holloway, "Model Estimates of M2 Internal Tide Energetics at the Hawaiian Ridge," J. Geophys. Res. **107** (C8), 3179 (2002).

17. W. Munk and C. Wunsch, "Abyssal Recipes II: Energetics of Tidal and Wind Mixing," Deep-Sea Res. **45**, 1977–2010 (1998).

18. A, A. Petrenko, B. H. Jones, T. D. Dickey, and P. Hamilton, "Internal Tide Effects on a Sewage Plume at Sand island, Hawaii," Cont. Shelf Res. **20**, 1–13 (2000).